

## Wave scattering by a dual cylindrical porous floating breakwater attached with a porous box

Kottala Panduranga\*, Santanu Koley

Department of Mathematics, Birla Institute of Technology and Science- Pilani, Hyderabad Campus, India-500078.

\* E-mail: p20180027@hyderabad.bits-pilani.ac.in

### Highlights

- Normal wave scattering by a dual cylindrical porous floating breakwater attached with porous box is studied.
- The physical problem is handled for solution using a boundary element method.
- To understand the effectiveness of the breakwater system, reflection, transmission and wave energy dissipation coefficients, wave forces acting on the breakwater are computed and analyzed for various values of wave and structural parameters.

### 1. Introduction

A floating breakwater is recognized as an effective wave-attenuation structure for protecting shorelines, marine facilities and providing the harbor tranquillity for ship activities within the harbor. Although the conventional breakwaters, such as bottom-standing rubble mound breakwaters, offer more protection than the floating breakwaters, the construction cost is more and also difficult to install, especially in the case of deep waters (Ji et al. (2019)). Therefore, the floating breakwaters represent an alternative solution to the conventional breakwaters. Due to these advantages over the last few years, the study of the wave interaction with the floating breakwaters has gained a great interest in coastal engineering. One such effective structure is a cylindrical floating breakwater system (Ozeren et al. (2011)). Ji et al. (2015) introduced a new type of floating breakwater consists of two parts such as rigid cylinders and flexible mesh cage to reduce the long waves' action. A series of model tests were conducted to investigate the effectiveness of the breakwater system. The results suggested that the proposed breakwater, i.e., a dual rigid cylinder and the flexible mesh cage with balls, shows better performance in reducing the wave transmission than the box type floating breakwaters, especially in the long-wave regime. Ji et al. (2017) studied the hydrodynamic behavior of a dual pontoon floating breakwater attached with flexible nets using the higher-order boundary element method based numerical solution technique. It was found that the heights of the vertical nets play a significant role in reducing the wave reflection and transmission by the breakwater system. However, the net height beyond 0.3 has no significant effect on the wave-blocking. Moreover, it is to be noted that in the aforementioned works, the cylindrical floating breakwaters are considered impermeable. Wang and Sun (2010) investigated experimentally that the porous floating breakwaters can effectively attenuate the incoming waves. In the present study, scattering of water waves by a dual cylindrical porous floating breakwater attached with the porous box is analyzed based on the linearized theory of water waves whilst the fluid flow within the porous cylinders is governed by the Sollitt and Cross model (Sollitt and Cross (1973)). The associate boundary value problem is handled for the solution using the boundary element method. Various results of physical interests are computed and analyzed to study the effects of various wave and structural parameters.

### 2. Mathematical formulation

In the present study, the problem is studied in the 2D Cartesian coordinate system under the assumption of linear water wave theory. The  $x$ -axis is taken in the horizontal direction and the  $z$ -axis is taken positive in the vertically upward direction. The schematic diagram for the present physical problem is as seen in Fig. 1. The floating breakwater occupies the region  $\{-l \leq x \leq l, -h < z < 0\}$ , due to the presence of the floating structure the physical domain is divided into four sub-regions  $R_j$  for  $j = 1, 2, 3, 4$  as shown in Fig. 1. The floating cylinders are identical in nature and the radius of the porous cylinders is  $a$  and the height and width of the porous rectangular box are  $h_1$  and  $b$  respectively. Assuming the fluid is incompressible, inviscid and irrotational and its motion simple-harmonic in time with the angular frequency  $\omega$ . These assumptions ensure that the existence of the velocity potential of the form  $\Phi_j(x, z, t) = \Re\{\phi_j(x, z) e^{-i\omega t}\}$ ,

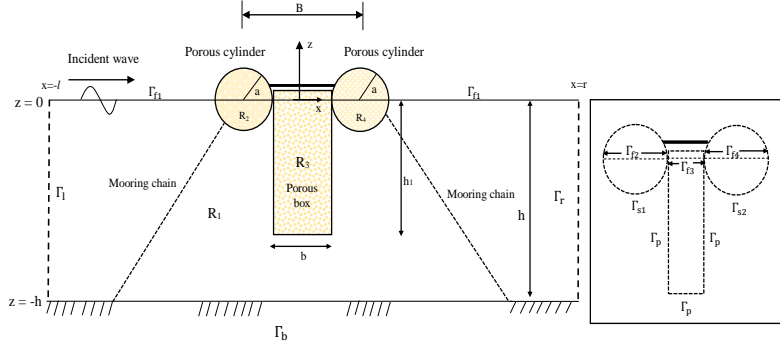


Fig. 1. Schematic diagram for the present physical problem.

where  $\Re$  denotes the real part of the complex function. Now, the spatial velocity potentials  $\phi_j$  satisfy the Laplace equation in the regions  $R_j$  for  $j = 1, 2, 3, 4$  as follows

$$\left( \frac{\partial^2}{\partial x^2} + \frac{\partial^2}{\partial z^2} \right) \phi_j = 0, \quad j = 1, 2, 3, 4. \quad (1)$$

along with the linearized free surface boundary condition

$$\frac{\partial \phi_j}{\partial z} - K(m_j + i f_j) \phi_j = 0, \quad \text{on } \Gamma_{f_j}, \quad j = 1, 2, 3, 4, \quad (2)$$

with  $K = \omega^2/g$ , and  $m_j, f_j$  being inertial and friction coefficients respectively (see Sollitt and Cross (1973), Koley et al. (2020) for more details). Further, the values of inertial coefficient  $m_1$  and friction coefficient  $f_1$  for open water region  $R_1$  are 1, 0 respectively. The boundary condition on the impermeable seabed is given by

$$\frac{\partial \phi_1}{\partial n} = 0, \quad \text{on } \Gamma_b. \quad (3)$$

Here,  $\partial/\partial n$  represents the outward drawn normal derivative from the corresponding boundary. At the interfaces between the regions  $R_1$  and  $R_j$ , ( $j = 2, 3, 4$ ), the continuity of pressure and mass flux hold and are given by (see Sollitt and Cross (1973))

$$\phi_1 = (m_j + i f_j) \phi_j, \quad \frac{\partial \phi_1}{\partial n} = -\epsilon_j \frac{\partial \phi_j}{\partial n}, \quad \text{on } \Gamma_{s1} \cup \Gamma_p \cup \Gamma_{s2}. \quad (4)$$

Here,  $\epsilon_j$  represents the porosity of the porous regions  $R_j$  for  $j = 2, 3, 4$ . Further,  $\Gamma_{s1}, \Gamma_p$  and  $\Gamma_{s2}$  represent the submerged boundaries of the regions  $R_2, R_3$  and  $R_4$  respectively. Finally, the far-field boundary conditions are given by

$$\begin{cases} \phi_1(x, z) = \phi_{inc}(x, z) + R_0 \phi_{inc}(-x, z), & \text{as } x \rightarrow -\infty, \\ \phi_1(x, z) = T_0 \phi_{inc}(x, z), & \text{as } x \rightarrow \infty, \end{cases} \quad (5)$$

where  $R_0$  and  $T_0$  are the unknown coefficients associated with the reflected and transmitted waves respectively. Theoretically, these far-field boundary conditions hold for  $x \rightarrow \pm\infty$ . However, for the sake of numerical computations, two auxiliary boundaries  $\Gamma_l$  and  $\Gamma_r$  are introduced at  $x = -l$  and  $x = r$ , which are far away from the structure (as seen in Fig. 1) so that the effect of local wave modes are negligible. In view of this, Eq. (5) are rewritten as

$$\begin{cases} \frac{\partial(\phi_1 - \phi_{inc})}{\partial n} - ik_0(\phi_1 - \phi_{inc}) = 0, & \text{on } \Gamma_l, \\ \frac{\partial \phi_1}{\partial n} - ik_0 \phi_1 = 0, & \text{on } \Gamma_r. \end{cases} \quad (6)$$

with  $\phi_{inc}$  being the incident wave potential and is given by  $\phi_{inc} = e^{ik_0} f_0(k_0, z)$  where the wave number  $k_0$  satisfying  $\omega^2 = gk_0 \tanh k_0 h$  and  $f_0(k_0, z) = \left( \frac{-igA}{\omega} \right) \frac{\cosh k_0(z+h)}{\cosh k_0 h}$  being the vertical eigenfunction in the open water region  $R_1$ .

### 3. Solution using boundary element method

The boundary value problem (BVP) in the four physical domain is converted into a system of integral equations using Green's integral theorem. Finally, matching the velocity and pressure on the interface boundaries between regions  $R_1$  and  $R_j$  for  $j = 2, 3, 4$ , the system of integral equations are handled for solution numerically.

#### Formulation of the integral equations

Applying Green's second identity to the velocity potential  $\phi(x, z)$  and the free space Green's function  $G(x, z; x_0, z_0)$  over the domain  $\Omega$  bounded by  $\Gamma$ , the following integral equation is obtained as

$$-\left( \begin{array}{c} \phi(x, z) \\ \frac{1}{2}\phi(x, z) \end{array} \right) = \int_{\Gamma} \left( \phi \frac{\partial G}{\partial n} - G \frac{\partial \phi}{\partial n} \right) d\Gamma, \quad \left( \begin{array}{c} \text{if } (x, z) \in \Omega \text{ but not on } \Gamma \\ \text{if } (x, z) \text{ on } \Gamma \end{array} \right). \quad (7)$$

In Eq. (7), the Green's function  $G(x, z; x_0, z_0)$  satisfies the governing differential equation (Eq. 1)

$$\left( \frac{\partial^2}{\partial x^2} + \frac{\partial^2}{\partial z^2} \right) G = \delta(x - x_0) \delta(z - z_0), \quad (8)$$

and is given by

$$G(x, z; x_0, z_0) = \frac{1}{2\pi} \ln r, \quad r = \sqrt{(x - x_0)^2 + (z - z_0)^2}, \quad (9)$$

The normal derivative of the Green's function  $G(x, z; x_0, z_0)$  is given by

$$\frac{\partial G}{\partial n} = \frac{1}{2\pi r} \frac{\partial r}{\partial n}. \quad (10)$$

Using the boundary conditions (2)-(6) in each of the regions  $R_j$  for  $j = 1, 2, 3, 4$ , the integral equation (7) is rewritten as

$$\begin{aligned} -\frac{1}{2}\phi_1 &+ \int_{\Gamma_1} \left( \frac{\partial G}{\partial n} - ik_0 G \right) \phi_1 d\Gamma + \int_{\Gamma_b} \phi_1 \frac{\partial G}{\partial n} d\Gamma + \int_{\Gamma_r} \left( \frac{\partial G}{\partial n} - ik_0 G \right) \phi_1 d\Gamma + \int_{\Gamma_{f1}} \left( \frac{\partial G}{\partial n} - KG \right) \phi_1 d\Gamma \\ &+ \int_{\Gamma_{s2} \cup \Gamma_p \cup \Gamma_{s1}} \left( \phi_1 \frac{\partial G}{\partial n} - G \frac{\partial \phi_1}{\partial n} \right) d\Gamma = \int_{\Gamma_1} \left( \frac{\partial \phi_{inc}}{\partial n} - ik_0 \phi_{inc} \right) G d\Gamma, \end{aligned} \quad (11)$$

$$-\frac{1}{2}\phi_2 + \int_{\Gamma_{s1}} \left( \frac{1}{(m_2 + if_2)} \phi_1 \frac{\partial G}{\partial n} + \frac{1}{\epsilon_2} G \frac{\partial \phi_1}{\partial n} \right) d\Gamma + \int_{\Gamma_{f2}} \left( \frac{\partial G}{\partial n} - K(m_2 + if_2) G \right) \phi_2 d\Gamma = 0, \quad (12)$$

$$-\frac{1}{2}\phi_3 + \int_{\Gamma_p} \left( \frac{1}{(m_3 + if_3)} \phi_1 \frac{\partial G}{\partial n} + \frac{1}{\epsilon_3} G \frac{\partial \phi_1}{\partial n} \right) d\Gamma + \int_{\Gamma_{f3}} \left( \frac{\partial G}{\partial n} - K(m_3 + if_3) G \right) \phi_3 d\Gamma = 0, \quad (13)$$

$$-\frac{1}{2}\phi_4 + \int_{\Gamma_{s2}} \left( \frac{1}{(m_4 + if_4)} \phi_1 \frac{\partial G}{\partial n} + \frac{1}{\epsilon_4} G \frac{\partial \phi_1}{\partial n} \right) d\Gamma + \int_{\Gamma_{f4}} \left( \frac{\partial G}{\partial n} - K(m_4 + if_4) G \right) \phi_4 d\Gamma = 0. \quad (14)$$

By discretizing the entire boundaries of the regions  $R_j$  for  $j = 1, 2, 3, 4$  into a finite number of segments called boundary elements and assuming  $\phi$  and  $\partial\phi/\partial n$  to be constant over each element (as in Koley et al. (2020)), the system of integral equations in Eqs. (11)-(14) are converted into a linear system of algebraic equations which are solved to get the unknown quantities of interest. Finally, the reflection, transmission, and wave energy dissipation coefficients

are calculated using the following formulae

$$K_r = |R_0|, \quad K_t = |T_0|, \quad K_D = (1 - K_r^2 - K_t^2). \quad (15)$$

#### 4. Results and Discussions

A MATLAB program is developed to investigate the effects of various wave and structural parameters on wave scattering by the dual floating porous cylinders attached with a porous box. Some of the computational results are plotted in Fig. 2.

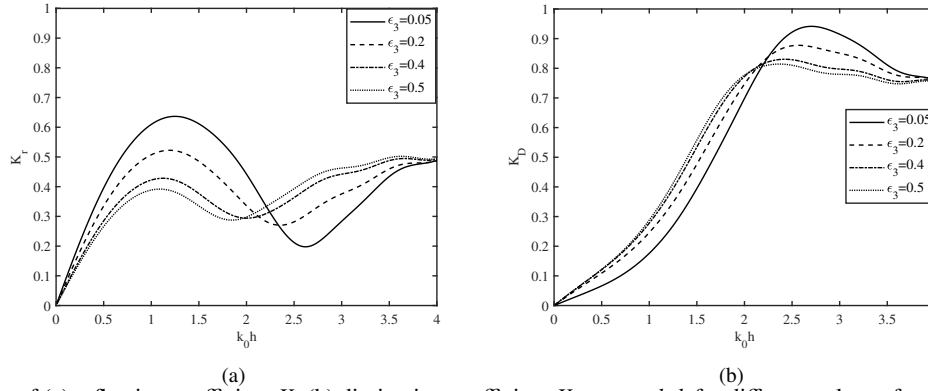


Fig. 2. Variation of (a) reflection coefficient  $K_r$  (b) dissipation coefficient  $K_D$  versus  $k_0 h$  for different values of porosity of the box  $\epsilon_3$  with  $\epsilon_2 = \epsilon_4 = 0.4$ ,  $f_2 = f_3 = f_4 = 1.0$ ,  $a = 0.25h$  and  $h_1 = h/2$ .

#### Acknowledgement

Koley S acknowledges the financial support received through the DST Project: DST/INSPIRE/04/2017/002460 to pursue this research work. Further, supports were received from BITS-Pilani, Hyderabad Campus through RIG project: BITS/GAU/RIG/2019/H0631 and Additional Competitive Research Grant: BITS/GAU/ACRG/2019/H0631.

#### References

#### References

- Ji, C., Cheng, Y., Yang, K., Oleg, G., 2017. Numerical and experimental investigation of hydrodynamic performance of a cylindrical dual pontoon-net floating breakwater. *Coastal Engineering* 129, 1–16.
- Ji, C.Y., Chen, X., Cui, J., Yuan, Z.M., Incecik, A., 2015. Experimental study of a new type of floating breakwater. *Ocean Engineering* 105, 295–303.
- Ji, C.Y., Zheng, R.S., Cui, J., Wang, Z.L., 2019. Experimental evaluation of wave transmission and dynamics of double-row floating breakwaters. *Journal of Waterway, Port, Coastal, and Ocean Engineering* 145, 04019013.
- Koley, S., Panduranga, K., Almashan, N., Neelamani, S., Al-Ragum, A., 2020. Numerical and experimental modeling of water wave interaction with rubble mound offshore porous breakwaters. *Ocean Engineering* 218, 108218.
- Ozeren, Y., Wren, D., Altinakar, M., Work, P., 2011. Experimental investigation of cylindrical floating breakwater performance with various mooring configurations. *Journal of waterway, port, coastal, and ocean engineering* 137, 300–309.
- Sollitt, C.K., Cross, R.H., 1973. Wave transmission through permeable breakwaters, in: *Coastal Engineering 1972*, pp. 1827–1846.
- Wang, H., Sun, Z., 2010. Experimental study of a porous floating breakwater. *Ocean Engineering* 37, 520–527.